

LiF:Mg,Cu,P BASED ENVIRONMENTAL DOSEMETER AND DOSE CALCULATION ALGORITHM

O. R. Perry†, M. Moscovitch‡, K. J. Velbeck§ and J. E. Rotunda§

†Lockheed Martin Idaho Technologies Company

PO Box 1625, Idaho Falls, ID 83415-4147, USA

‡Department of Radiation Medicine, Georgetown University School of Medicine

3800 Reservoir Rd., N.W., Washington, DC 20007, USA

§BICRON ♦ NE Div. of St. Gobain Industrial Ceramics, Inc.

6801 Cochran Rd., Solon, OH 44139, USA

Abstract — The development is described of a new environmental TLD dosimeter badge and dose computation algorithm based on the new LiF:Mg,Cu,P material. LiF:Mg,Cu,P, with its high sensitivity, tissue equivalence, energy independence, and low fading characteristics, is a natural choice for environmental dosimetry. The badge consists of a card and a plastic holder. The card contains four LiF:Mg,Cu,P elements encapsulated in Teflon. The elements are all 3.2 mm square and 0.4 mm thick. The badge is symmetrical and uses four filters to discriminate low and high energy photons and to determine directional dose equivalent, $H'(0.07, \alpha)$, and ambient dose equivalent, $H^*(10)$. Extensive data were taken based on irradiations of 920 dosimeters to both single and mixed fields of photons and betas. In addition, angular incidence data of various fields were taken. The approach to the algorithm is empirical and is based on these data. While most algorithms are based solely on perpendicular incidence exposure, this algorithm is being developed to account for the angular response of the dosimeter. The algorithm for perpendicular irradiation is presented. The angular incidence portion of the algorithm is in development. The dosimeter is designed to meet the criteria of the new draft standard ANSI N13.29, 'Environmental Dosimetry Performance — Criteria for Testing'.

INTRODUCTION

A new environmental standard, ANSI N13.29 (draft), is geared toward monitoring human exposure to ionising radiation in the environment. In the spirit of this draft, a new environmental algorithm is being developed to meet the criteria of that standard. The algorithm, along with its associated dosimeter, will enable one to report directional dose equivalent, $H'(0.07, \alpha)$, and ambient dose equivalent, $H^*(10)$. Work toward the development of the algorithm, presented in this paper, includes photon energy response, beta energy response, mixed field energy response, and fading.

The dosimeter is the Harshaw Type 8855, containing four LiF:Mg,Cu,P elements. The TL measurements were taken at the Idaho National Engineering and Environmental Laboratory (INEEL), the irradiations were performed at Battelle Pacific Northwest Laboratories, and an algorithm was developed for perpendicular incidence exposure. A more robust algorithm which takes into account the angular dependence of the dosimeter is under development at BICRON ♦ NE and will be published later.

DOSEMETER

The dosimeter is based on the LiF:Mg,Cu,P phosphor. It was chosen for its high sensitivity (about ten times higher than LiF:Mg,Ti), a relatively flat photon energy response, near tissue equivalence, and negligible fading. These features makes a LiF:Mg,Cu,P-based dosimeter ideal for environmental work.

The Type 8855 Dosimeter is composed of a card and

holder (Figure 1). The card is made of aluminium and contains four LiF:Mg,Cu,P elements in a Teflon encapsulation. Each element is 3.2 mm square by 0.4 mm thick. A label with a barcode and numeric identification is attached to the card. The card is inserted into a holder which contains symmetric filtration over the front and back of each element. The filtration covering Element

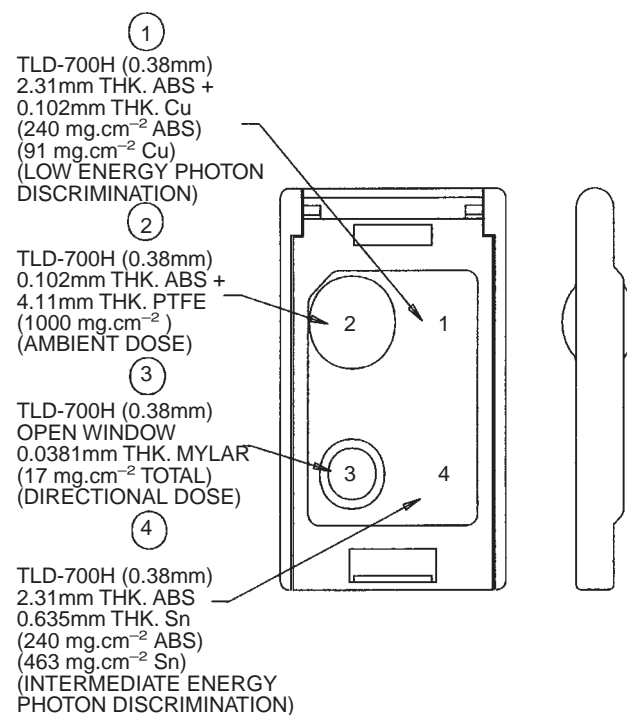


Figure 1. Type 8855 dosimeter.

Number 1 consists of 91 mg.cm⁻² Cu + 240 mg.cm⁻² ABS plastic and is used for low energy photon discrimination. Element Number 2 filtration consists of 1000 mg.cm⁻² PTFE + ABS plastic and is used for ambient dose measurement. Element Number 3 has 17 mg.cm⁻² of Mylar plus PTFE encapsulation, and is used for directional dose measurement. Element Number 4 filtration consists of 464 mg.cm⁻² Sn + 240 mg.cm⁻² ABS plastic and is used for intermediate energy photon discrimination. The card identification is visible through a red filter window located in the centre of the front side of the holder.

READER

The TL measurements were performed using a Harshaw Model 6600 Automatic TLD Card Reader. The reader is capable of reading two hundred four-element TLD cards in one pre-programmed cycle. The reader uses hot nitrogen gas for non-contact heat transfer. The heating method employs a closely controlled, linearly ramped time temperature profile⁽¹⁾. Card identification is automatically read and recorded. The reader is calibrated using a local reference source. Each dosimeter card used in the testing is pre-calibrated. Element correction coefficients (ECCs), determined at the time of pre-calibration, are applied during the test readouts⁽²⁾. Glow curves were recorded using a preheat of 50°C for 0 s, a heating rate of 15°C.s⁻¹, a maximum temperature

of 260°C, and an anneal of 260°C for 10 s. Typical glow curves as read on the Model 6600 are shown in Figure 2. Note that the lower temperature peaks are absent because of the long fading time involved.

TEST DESCRIPTION

Approximately 920 dosimeters were irradiated and read for energy response testing purposes. Table 1 summarises the tests performed. For photons and betas, all delivered doses were of the order of 2.00 mGy. All irradiations were incident to the dosimeter face containing the barcode window. This position was also considered the zero angle position for the angular testing. For the angular dependence testing, only unique angles of incidence were used based on the symmetric nature of the dosimeter.

Irradiations

All of the energy response data presented is based on the irradiations performed free-in-air at Battelle Pacific Northwest Laboratories. The Battelle laboratory is a recognised secondary irradiation laboratory with sources traceable to the National Institute for Standards and Technology (NIST). Table 2 summarises the radiation techniques involved.

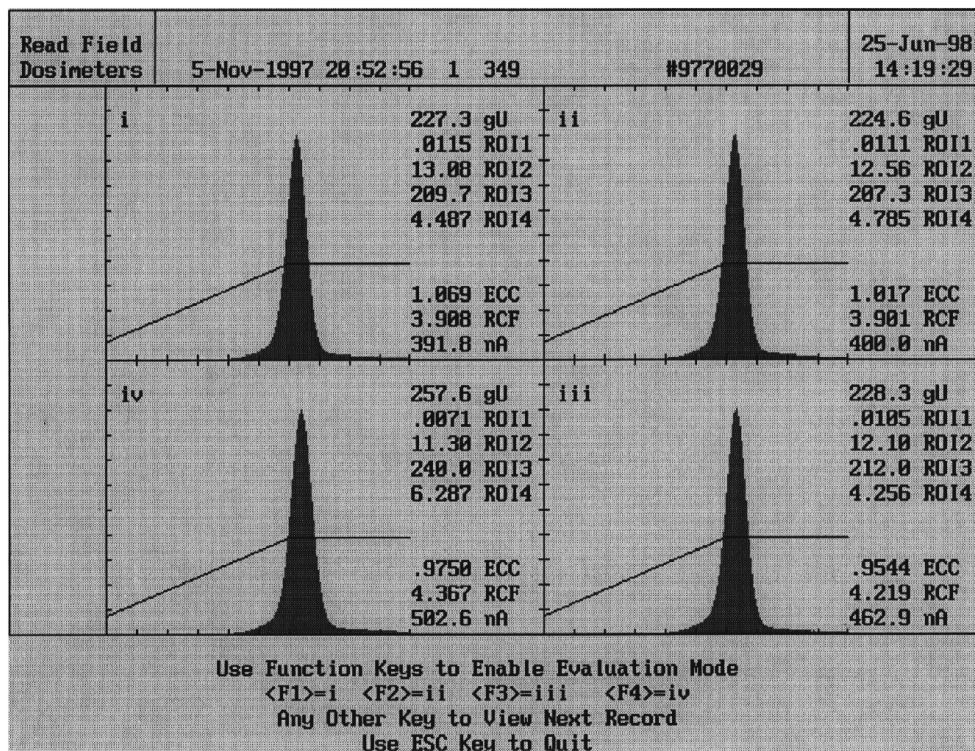


Figure 2. LiF:Mg,Cu,P glow curves.

TESTING RESULTS

Dosemeter response — photon and beta pure fields

Shown in Table 3 is a compilation of the response in unit gU of each dosimeter element, to each pure radiation field type. The gU is a generic unit (a unit referenced to a stable calibration source). Each data point is based on the reading of five dosimeters. The relative standard deviation of the five readings is included.

Photon energy response — pure fields

The graph in Figure 3 represents the photon energy response of each of the elements in the dosimeter referenced to ^{137}Cs for pure fields. The results show that with light filtration, such as is the case in Element 3, the energy response of the dosimeter is relatively flat. Combined with the response of elements with heavier filtration, ratios of elements will give useful information

Table 1. Test description.

Test	Test description	Radiation type(s)
Angular dependence	<i>Vertical angles</i> 0°, 30°, 60°, 75°, 90°, 270°, 285°, 300°, 330°	M30, H100, H150, H250, ^{137}Cs , ^{241}Am , $^{90}\text{Sr-}^{90}\text{Y}$
	<i>Horizontal angles</i> 0°, 30°, 60°, 75°, 90°, 270°, 285°, 300°, 330°	M30, H100, H150, H250, ^{137}Cs , ^{241}Am , $^{90}\text{Sr-}^{90}\text{Y}$
Pure fields	Low energy photon, High energy photons, Betas	M30, M100, H40, H50, H100, H150, H200, H250, ^{137}Cs , ^{60}Co , ^{204}Tl , ^{241}Am , $^{90}\text{Sr-}^{90}\text{Y}$, DU
Mixed fields	1:1 Ratio	^{137}Cs + M30, M100, H40, H50, H100, H150, H200, H250, ^{241}Am $^{90}\text{Sr-}^{90}\text{Y}$, ^{204}Tl , DU
	1:1 Ratio	DU + M30, M100, H40, H50, H100, H150, H200, H250, ^{241}Am
	1:1 Ratio	^{204}Tl + M30, M100, H40, H50, H100, H150, H200, H250, ^{241}Am
	1:1 Ratio	$^{90}\text{Sr-}^{90}\text{Y}$ + M30, M100, H40, H50, H100, H150, H200, H250, ^{241}Am
1:1 Ratio	^{60}Co + M30, M100, H40, H50, H100, H150, H200, H250, ^{241}Am , $^{90}\text{Sr-}^{90}\text{Y}$, ^{204}Tl , DU	

as to what energy is being measured in a blind test situation. This is an integral part of the algorithm development.

Angular dependence — pure fields

The Type 8855 dosimeters were irradiated in open air on a special mounting frame which rotates the dosimeters around vertical and horizontal axes (see Figure 4). Low energy X rays (M30, H100, H150, H250), gamma (^{241}Am , ^{137}Cs , ^{60}Co), and beta fields ($^{90}\text{Sr-}^{90}\text{Y}$) were measured. Because of the symmetric nature of the holder, measurements were made over 180° around only one face of the holder. Nine different angles were measured around each of the two axis. The data show that the angular dependence is relatively low for angles within 60° of the zero reference. The graphs in Figures 5 and 6 depict the angular dependence of the dosimeter in typical photon (^{137}Cs) and beta ($^{90}\text{Sr-}^{90}\text{Y}$) fields, respectively. As expected, the penetrating radiations such as ^{137}Cs have less angular dependence than the non-penetrating radiations such as $^{90}\text{Sr-}^{90}\text{Y}$.

Mixed photon and beta fields

Shown in Table 4 is the response of each of the four elements in a card to various combinations of photon and beta mixed fields. Through the determination of the appropriate ratios of elements, correction values can be determined and applied in the algorithm. In addition, limits of measurements can be established.

Fading

A test was performed to determine the response degradation due to loss of sensitivity (pre-exposure

Table 2. Irradiation types.

	Radiation field	Energy (keV)
X ray	M30 Technique	20
	H40 Technique	33
	H50 Technique	38
	M100 Technique	51
	H100 Technique	80
	H150 Technique	120
Gamma	H200 Technique	166
	H250 Technique	211
	^{241}Am	60
Beta	^{137}Cs	662
	^{60}Co	1250
	^{204}Tl	760
	$^{90}\text{Sr-}^{90}\text{Y}$	2300
	Depleted uranium	2300

fade) and fading (post-exposure fade) over time. The test involved preparing a set of dosimeters by clearing, waiting a predetermined amount of time, irradiating the dosimeter to 10 mGy, waiting a predetermined amount of time and then reading the dosimeter. For this test the pre-exposure time was set equal to the post-exposure time. Results show less than 4% fading in 90 days (referenced to two days). Tests are in progress to determine fading using a preheat during the read cycle. By applying this preheat, it is predicted that fading can be reduced to near zero per cent.

ALGORITHM DEVELOPMENT

A neural-network technique⁽³⁾ was employed in this

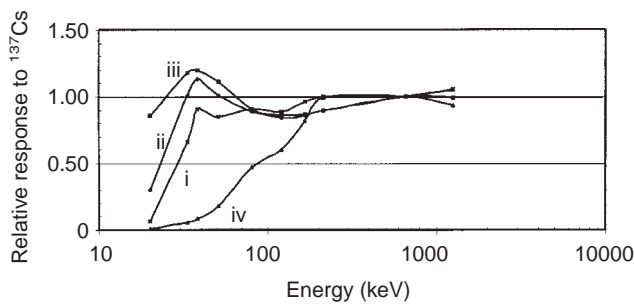


Figure 3. Photon energy response of 8855 dosimeter. Elements i-iv indicated on curves.

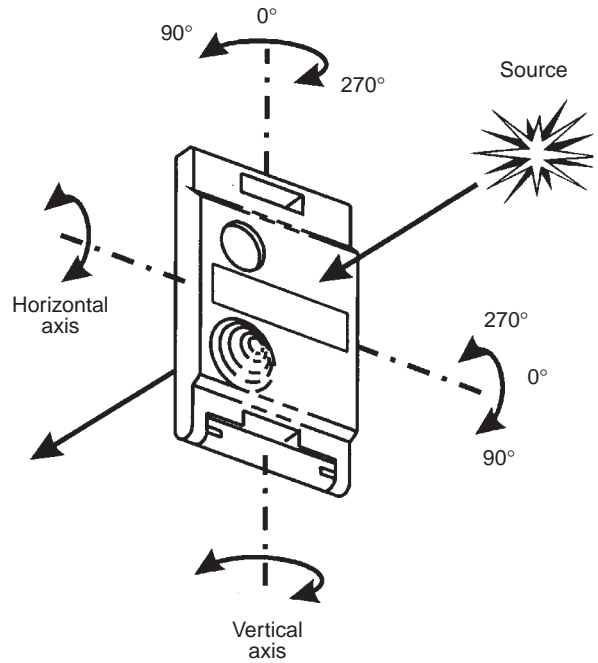


Figure 4. Angular dependence set-up.

Table 3. TLD element response — pure fields.

		TLD element response Pure photon and beta field							
		i		ii		iii		iv	
Photons	(mGy)	gU	σ(%)	gU	σ(%)	gU	σ(%)	gU	σ(%)
M30	2.0	14.21	2.56	62.93	1.03	175.9	1.24	1.77	46.4
M100	2.0	179.5	1.55	210.5	1.55	229.9	1.07	41.05	15.2
H40	2.0	137.7	1.65	209.9	1.37	242.3	1.40	12.66	15.9
H50	2.0	190.7	6.23	235.4	6.85	246.0	8.83	20.99	12.3
H100	2.0	191.2	175	185.0	1.55	186.1	3.04	110.4	12.1
H150	2.0	187.1	2.23	175.6	1.96	175.9	3.55	141.5	4.91
H200	2.0	201.0	1.40	187.0	3.39	176.9	2.93	192.0	3.69
H250	2.0	210.3	1.53	185.0	2.37	183.6	2.97	230.7	2.75
²⁴¹ Am	2.0	214.1	2.43	217.3	1.60	223.5	1.50	54.25	29.2
¹³⁷ Cs	2.0	209.8	1.15	207.0	0.98	204.6	1.88	233.6	1.39
⁶⁰ Co	2.0	221.5	0.87	216.5	0.88	203.5	1.13	218.5	1.32
		i		ii		iii		iv	
Betas		gU	σ(%)	gU	σ(%)	gU	σ(%)	gU	σ(%)
⁹⁰ S- ⁹⁰ Y	2.0	52.54	3.81	3.71	11.08	211.0	2.25	5.28	14.3
DU	2.0	20.60	2.33	4.80	8.60	117.6	1.43	5.67	6.02
²⁰⁴ Tl	2.0	0	—	0	—	88.75	5.40	0	—

sistent with the requirements of the new environmental dosimetry draft standard (ANSI N13.29-draft). The algorithm does not cover non-perpendicular radiation. The following briefly describes the basic ideas behind this algorithm.

In short, neural networks⁽⁵⁾ are a family of computational methods inspired by the functionality of living neurons. Unlike conventional computing, a neural network has the capability to learn from its own experience and produce its own solution. The basic component of a neural network is a node, and the network typically consists of an input layer of nodes, an output layer and possibly one or more hidden layers in between. The network is connected by the links between the nodes; these links carry specific weights. The actual intelligence of the network lies in the weighting factors, which are

determined by training the network using a variety of input/output data pairs. The weights are being continuously updated by a learning algorithm until the network learns to associate between the input and the appropriate output. The learning algorithm is based on least squares to minimise the network error, which is defined as the difference between the actual output and the desired output.

In the application of neural networks to personnel or environmental dosimetry, the inputs of the training pairs are the TL signals from the various elements, L1, L2, L3 and L4, and the outputs are the desired quantities, for example, the air kerma, the ambient and the directional dose equivalent. The input/output training sets are generated by exposing dosimeters to a variety of mixed photon-beta fields. The training set consists of a variety

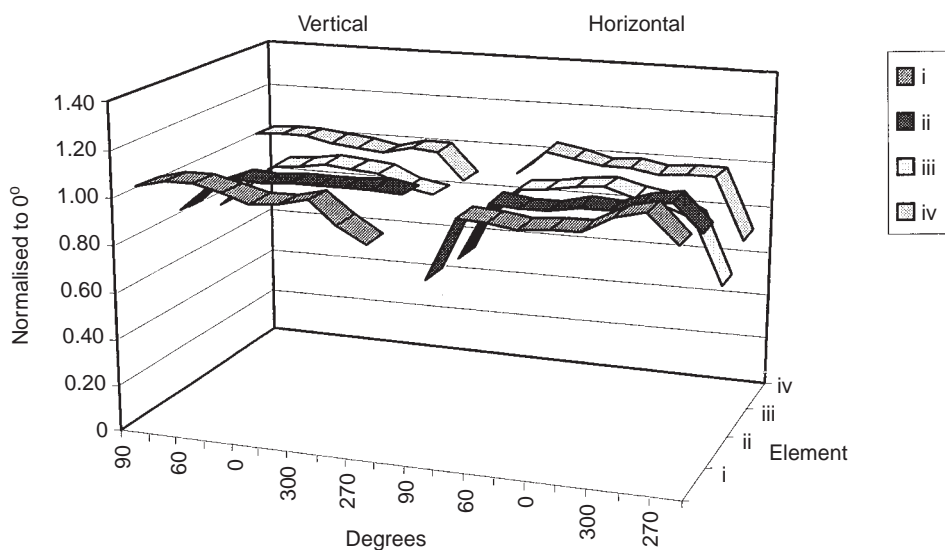


Figure 5. ¹³⁷Cs angular dependence.

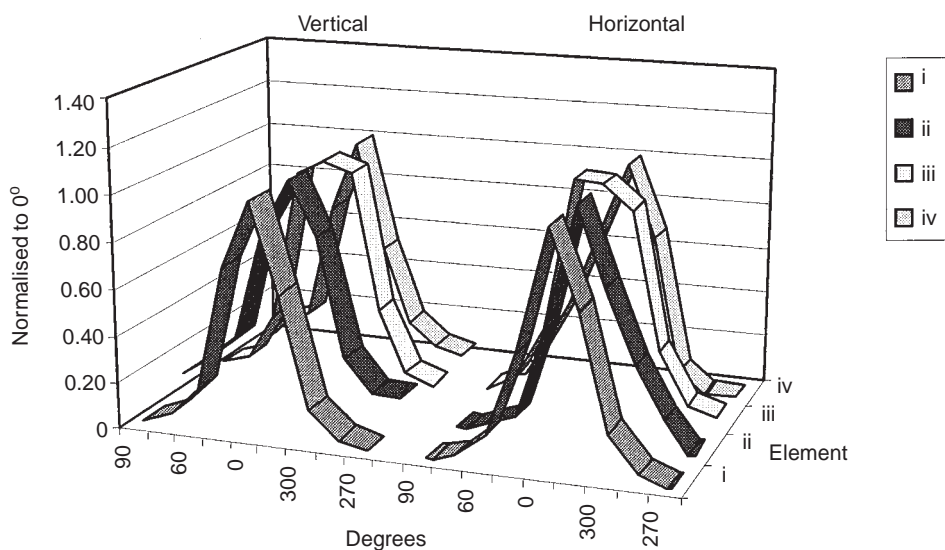


Figure 6. ⁹⁰Sr-⁹⁰Y angular dependence.

Table 4. TLD element response — mixed photon and beta field.

Irradiation		Irradiation		TLD element response Mixed photon and beta field							
				i		ii		iii		iv	
(mGy)	(mGy)	gU	σ (%)	gU	σ (%)	gU	σ (%)	gU	σ (%)		
¹³⁷ Cs	2.00	M30	2.01	220.5	1.02	266.4	1.34	374.7	0.92	232.3	1.48
		M100	2.00	378.8	1.14	408.9	1.54	421.3	1.39	264.6	1.98
		H40	2.00	344.0	1.16	412.5	1.64	444.2	0.99	246.8	1.37
		H50	2.01	391.8	3.03	438.2	3.94	440.7	5.04	247.3	2.18
		H100	2.01	395.9	1.12	386.9	1.28	381.6	2.89	337.7	4.53
		H150	2.01	386.3	0.87	373.0	1.23	373.1	1.00	365.0	1.46
		H200	2.00	403.7	1.00	379.1	1.64	376.4	1.40	418.9	2.54
		H250	2.01	413.8	1.48	386.4	2.32	373.3	1.93	451.6	2.11
		²⁴¹ Am	2.00	414.7	2.15	409.7	1.49	413.5	0.78	287.2	4.46
		⁶⁰ Co	2.00	M30	2.01	238.0	1.11	279.3	1.05	382.8	1.61
M100	2.01			402.5	0.85	427.6	2.74	428.4	3.27	250.2	3.68
H40	2.00			360.5	2.16	424.8	1.11	445.1	1.93	232.9	2.20
H50	2.00			413.9	3.09	452.3	2.59	450.5	4.11	240.9	1.62
H100	2.00			422.1	2.47	404.7	0.91	386.8	3.15	320.1	3.64
H150	2.01			411.8	2.21	392.1	1.66	376.0	2.46	360.8	3.83
H200	2.00			422.4	1.35	394.2	0.39	381.2	1.40	417.6	2.19
H250	2.01			437.7	1.69	399.1	1.00	384.0	3.02	449.9	2.00
²⁴¹ Am	2.00			424.4	1.65	423.6	2.06	423.1	0.39	262.5	4.82
DU	2.00			M30	2.01	34.4	1.92	65.6	1.03	282.1	0.98
		M100	2.00	192.4	1.31	209.7	1.27	335.5	1.66	45.0	15.97
		H40	2.00	153.4	1.74	210.6	1.33	346.9	1.68	19.3	14.90
		H50	2.01	207.6	3.85	244.0	3.98	351.6	6.95	25.9	12.26
		H100	2.00	205.5	2.79	186.5	2.33	291.3	1.03	96.2	17.14
		H150	2.00	200.4	1.79	175.5	1.64	282.1	1.81	142.9	4.37
		H200	2.00	216.8	2.83	180.3	1.89	281.0	2.06	192.5	5.90
		H250	2.01	222.9	2.16	185.5	2.60	289.5	2.21	219.3	4.32
		²⁴¹ Am	2.00	225.2	2.14	216.0	2.09	323.7	2.19	60.4	20.76
		²⁰⁴ Tl	2.00	M30	2.01	14.4	3.39	63.2	1.98	263.5	2.45
M100	2.00			175.3	1.00	210.2	2.03	317.3	2.96	42.0	19.88
H40	2.00			136.4	2.34	207.1	1.18	329.1	1.17	14.8	7.68
H50	2.01			187.5	5.64	231.9	5.11	326.9	6.26	19.2	23.47
H100	2.00			187.7	1.94	183.7	1.57	275.0	0.84	106.4	13.23
H150	2.01			184.8	2.37	174.8	1.69	263.2	1.30	147.5	2.72
H200	2.01			201.0	2.85	177.6	1.89	266.4	0.47	194.0	6.15
H250	2.00			207.5	1.78	181.2	2.27	271.3	1.38	223.9	4.08
²⁴¹ Am	2.00			211.4	2.00	214.3	1.32	304.4	2.14	59.0	17.08
⁹⁰ Sr- ⁹⁰ Y	1.94			M30	2.01	66.2	3.91	66.9	1.97	381.4	1.82
		M100	2.00	226.8	1.29	212.7	2.36	435.0	1.31	42.4	14.59
		H40	2.00	186.1	1.58	210.2	1.28	443.2	2.12	19.2	3.31
		H50	2.00	237.2	4.22	238.2	6.19	445.9	3.87	21.3	21.87
		H100	2.00	238.1	1.60	186.4	2.37	386.6	2.26	114.8	6.01
		H150	2.01	235.5	1.02	176.7	1.72	384.0	2.37	143.5	9.70
		H200	2.00	246.9	1.14	179.3	1.60	384.0	2.93	194.3	2.94
		H250	2.00	259.5	2.81	183.1	2.80	379.9	2.63	230.6	5.94
		²⁴¹ Am	2.00	258.5	4.13	216.0	2.16	421.1	1.68	65.2	8.07
		¹³⁷ Cs	2.00	⁹⁰ Sr- ⁹⁰ Y	1.94	253.1	1.55	206.6	1.70	405.7	1.76
²⁰⁴ Tl	2.00			202.9	2.71	203.7	0.87	291.7	1.73	225.0	3.13
DU	2.00			224.4	1.45	2.0	1.10	313.5	1.84	234.0	1.90
⁶⁰ Co	2.00	⁹⁰ Y	1.94	267.9	2.89	212.5	0.69	403.9	2.26	220.2	1.00
		²⁰⁴ Tl	2.00	210.0	1.23	205.7	0.59	282.2	1.22	207.9	2.11
		DU	2.00	237.3	0.70	214.6	0.71	313.6	1.36	220.5	1.53

of energies as well as mixtures, types and angles of incidence. Adding more types of exposures in the training set improves the learning process and usually results in a ‘smarter’ network, leading to a better and more accurate dose algorithm. The concept of functional links⁽⁶⁾ has been adopted to create a functional link network (FLN) and apply it to the development of the dose algorithm. The FLN enables the increase of the dimensionality of the input space (the number of nodes in the input layer) and results in a simple network without hidden layers. For a LiF:Mg,Cu,P-based four-element dosimeter, the functional link method described below was found to produce excellent results in terms of accuracy and precision. The input to the network consists of the following element ratios: $X_1 = L_1/L_4$; $X_2 = L_3/L_2$; $X_3 = L_3/L_1$. Each of these ratios is passed through four functional links. In addition, there is a ‘true’ node which is always ‘on’ and the weight leading from this node provides a constant bias term. The functions used in this network are: $f_i = [\log(x)]^i$, $i = 1, \dots, 4$. The weights associated with the various links are $\{W_{ij}\}$, $i = 1, \dots, 4$ and $j = 1, \dots, 3$. The air kerma conversion factor used to calculate the air kerma is given by the following function:

$$K = \sum_{i=1}^4 \sum_{j=1}^3 W_{ij} f_i(X_j) + C$$

The same concept applies to other calibration values used to calculate the ambient and directional dose, but the different input and link functions are chosen. The weighting coefficients are calculated by minimising the difference between the desired output and the actual output of the network. This equation is linear, i.e. it can be expressed as a linear combination of the logarithmic functions and their powers. This linearity makes it possible to use a variety of the multiple regression techniques⁽⁷⁾.

Formalisation

The actual form of the algorithm developed by this process is as follows.

(1) Obtain input data

Step a. Subtract background–TL signals of four elements in unit μG

$$TL_1, TL_2, TL_3 \text{ and } TL_4$$

Step b. ¹³⁷Cs response–TL signals of four elements in unit $\text{gU}\cdot\text{mGy}^{-1}$

$$TC(1), TC(2), TC(3) \text{ and } TC(4)$$

Step c. ¹³⁷Cs relative signals of four elements in unit mGy

$$L_1 = TL_1/TC(1)$$

$$L_2 = TL_2/TC(2)$$

$$L_3 = TL_3/TC(3)$$

$$L_4 = TL_4/TC(4)$$

If $L_i < 0$, set $L_i = 0.001$

(2) Calculate beta TL signal (in unit mGy)

$$BTL = L_3 - L_2$$

(3) Decide if a beta field present

If $|\frac{BTL}{L_2}| > 0.2$, yes, there is a beta field.

(4) Calculate L_2/L_4

If, $\frac{L_2}{L_4} > 15$, set $\frac{L_2}{L_4} = 15$

If $\frac{L_2}{L_4} < 1$, set $\frac{L_2}{L_4} = 1$

Else, calculate L_2/L_4 .

(5) Calculate ratios

$$X_1 = L_1/L_4$$

$$X_2 = L_3/L_2$$

$$X_3 = L_3/L_1$$

(6) Functional links for air kerma factor

$$f_1(X_1) = \log(X_1) \quad f_1(X_2) = \log(X_2)$$

$$f_1(X_3) = \log(X_3)$$

$$f_2(X_1) = \log^2(X_1) \quad f_2(X_2) = \log^2(X_2)$$

$$f_2(X_3) = \log^2(X_3)$$

$$f_3(X_1) = \log^3(X_1) \quad f_3(X_2) = \log^3(X_2)$$

$$f_3(X_3) = \log^3(X_3)$$

$$f_4(X_1) = \log^4(X_1) \quad f_4(X_2) = \log^4(X_2)$$

$$f_4(X_3) = \log^4(X_3)$$

(7) Calculate air kerma factor K

Case 1. Only low energy photon fields (33 – 80 keV),

$$K = 1.867 f_1(X_1) - 4.365 f_1(X_2) + 0.9099 f_1(X_3)$$

$$- 3.684 f_2(X_1) + 282.5 f_2(X_2) - 13.36 f_2(X_3)$$

$$+ 3.996 f_3(X_1) - 9292 f_3(X_2) + 146.5 f_4(X_3)$$

$$- 1.701 f_4(X_1) + 83614 f_4(X_2) - 396.7 f_4(X_3)$$

$$+ 0.6003$$

Case 2. Intermediate high energy photon (80 – 1250 keV) or any mixed photon fields,

$$K = 0.1157 f_1(X_1) - 4.025 f_1(X_2) + 1.802 f_1(X_3)$$

$$- 13.32 f_2(X_1) + 71.94 f_2(X_2) - 6.470 f_2(X_3)$$

$$+ 90.29 f_3(X_1) + 1183 f_3(X_2) - 65.75 f_4(X_3)$$

$$- 150.3 f_4(X_1) - 36145 f_4(X_2) + 456.1 f_4(X_3)$$

$$+ 0.9844$$

If $K < 0.75$, set $K = 0.9$.

Case 3. Pure beta or mixed photon + beta fields,

$$K = -0.6551 f_1(X_1) - 4.410 f_1(X_2) - 4.539 f_1(X_3) + 1.579 f_2(X_1) - 28.74 f_2(X_2) + 42.54 f_2(X_3) - 0.6267 f_3(X_1) + 239.7 f_3(X_2) - 1.045 f_4(X_3) - 0.1719 f_4(X_1) - 405.2 f_4(X_2) + 150.7 f_4(X_3) + 1.833$$

If $K < 0.89$, set $K = 0.87$

If $0.89 < K < 0.98$, set $K = 1$.

(8) Calculate ambient and directional dose factors a and d (in unit mSv/mGy)

Case 1. Only low energy photon fields (33 – 80 keV),

$$a = -81.74 \log(L_2/L_4) + 370.4 \log^2(L_2/L_4) - 823.8 \log^3(L_2/L_4) + 955.8 \log^4(L_2/L_4) - 554.8 \log^5(L_2/L_4) + 127.0 \log^6(L_2/L_4) + 8.629$$

$$d = -46.09 \log(L_2/L_4) + 211.8 \log^2(L_2/L_4) - 478.2 \log^3(L_2/L_4) + 563.2 \log^4(L_2/L_4) - 331.8 \log^5(L_2/L_4) + 77.10 \log^6(L_2/L_4) + 5.452$$

Case 2. Intermediate high energy photon (80 – 125 KeV) or any mixed photon fields,

$$a = -1.973 \log(L_2/L_4) + 24.08 \log^2(L_2/L_4) + 288.2 \log^3(L_2/L_4) - 3653 \log^4(L_2/L_4) + 12329 \log^5(L_2/L_4) - 13407 \log^6(L_2/L_4) + 1.309$$

$$d = -1.377 \log(L_2/L_4) + 33.99 \log^2(L_2/L_4) - 33.01 \log^3(L_2/L_4) - 997.8 \log^4(L_2/L_4) + 3571 \log^5(L_2/L_4) - 3298 \log^6(L_2/L_4) + 1.304$$

Case 3. Pure beta or mixed photon + beta fields,

$$a = -0.6470 \log(L_2/L_4) + 21.07 \log^2(L_2/L_4) - 79.12 \log^3(L_2/L_4) + 120.8 \log^4(L_2/L_4) - 84.34 \log^5(L_2/L_4) + 22.31 \log^6(L_2/L_4) + 1.288$$

$$d = -0.731 \log(L_2/L_4) + 24.36 \log^2(L_2/L_4) - 87.08 \log^3(L_2/L_4) + 125.9 \log^4(L_2/L_4) - 83.81 \log^5(L_2/L_4) + 21.31 \log^6(L_2/L_4) + 1.321$$

(9) Calculate dose quantities

H7 beta directional dose equivalent (mSv)

$$H7 = 0.574 BTL - 0.429 BTL^2 + 0.093 BTL^3 + 1.76$$

H7 = 0, if no beta signal present.

K_a air kerma for photons (mGy)

$$K_a = L_2/K$$

H(0.07) photon directional dose equivalent (mSv)

$$H(0.07) = dK_a$$

H(10) photon ambient dose equivalent (mSv)

$$H(10) = aK_a$$

H'(0.07) total directional dose equivalent (mSv)

$$H'(0.07) = H(0.07) + H7$$

H*(10) total ambient dose equivalent (mSv)

$$H^*(10) = H(10)$$

The conversion factors $C'_k(0.07)$ and $C^*_k(10)$ used in the algorithm are those developed by Soares and Martin⁽⁸⁾.

RESULTS

The algorithm was tested by processing all of the field card readings through it. The results, in Figure 7, show that all $|B| + S$ values are well within the 50% tolerance limit required by ANSI N13.29; in fact, most were under 10% and none exceeded 30%.

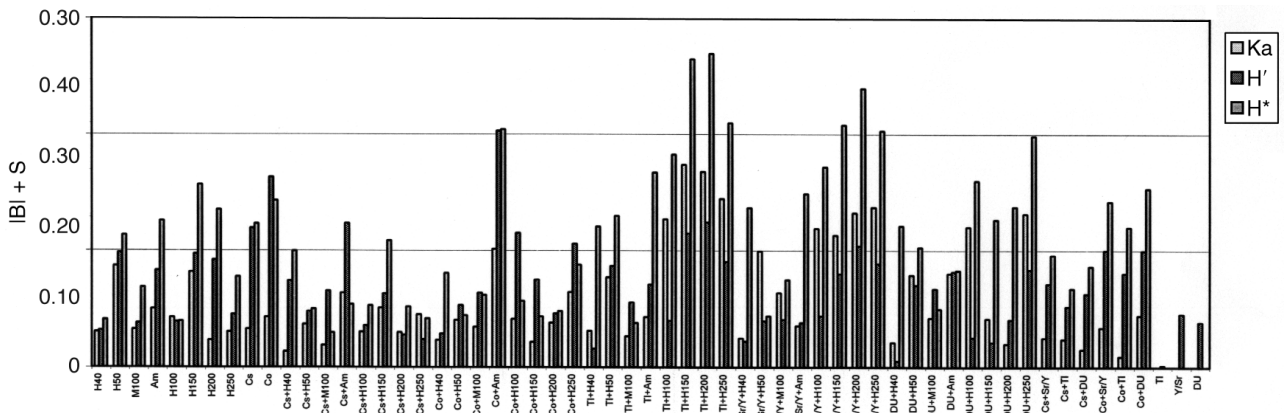


Figure 7. Preliminary algorithm test results.

CONCLUSION

Extensive testing with positive results has shown that an integrated system comprising a Harshaw Model 6600

TLD Reader, high sensitivity LiF:Mg,Cu,P dosimeters, and the Harshaw neural network dose computational algorithm is capable of reporting doses well within the standards required by ANSI N13.29.

REFERENCES

1. Velbeck, K. J., Szalanczy, A. and Bruml, W. *An Automatic, Medium Capacity, Controlled Linear Heating TLD System Methodology for Performance Evaluation*. (Unpublished).
2. Moscovitch, M., Chamberlain, J. and Velbeck, K. J. *Dose Determination Algorithm for a Nearly Tissue-Equivalent Multi-Element Thermoluminescent Dosimeter*. In: Proc. 2nd Conf. on Radiation Protection and Dosimetry, Orlando, FL. ORNL/TM-10971, pp. 48–59 (1988).
3. Moscovitch, M. and Rotunda, J. E. *Multi-element Dosimetry System Using Neural Network*. US Patent No 5,572,028 (1996).
4. Moscovitch, M. *Personnel Dosimetry Using LiF:Mg,Cu,P*. Radiat. Prot. Dosim. **85**(1–4), 49–56 (This issue) (1999).
5. Clark, J. W. *Neural Network Modelling*. Phys. Med. Biol. **36**, 1259–1317 (1991).
6. Freeman, J. A. *Simulating Neural Networks with Mathematics* (Addison-Wesley) (1994).
7. Neter, J., Wasserman, W. and Kutner, M. H. *Applied Linear Statistical Models*, 2nd edn, (Homewood, Illinois: Irwin) (1985).
8. Soares, C. *A Comprehensive Set of Conversion Coefficients for Photons*. Presented at BICRON ♦ NE TLD Users Symposium, Changes and Opportunities in Dosimetry, Las Vegas, 13–17 March 1995.